



Biological productivity regime and associated N cycling

A. J. Cavagna et al.

Biological productivity regime and associated N cycling in the vicinity of Kerguelen Island area, Southern Ocean

A. J. Cavagna¹, F. Fripiat¹, M. Elskens¹, F. Dehairs¹, P. Mangion², L. Chirurgien³, I. Closset⁴, M. Lasbleiz³, L. Flores–Leiva^{5,6,7}, D. Cardinal⁴, K. Leblanc³, C. Fernandez^{5,6,7,8}, D. Lefèvre³, L. Oriol⁸, S. Blain⁸, and B. Quéguiner³

¹Analytical, Environmental and Geo-Chemistry dept. (AMGC), Earth System Sciences Research Group, Vrije Universiteit Brussel, Brussels, Belgium

²Centre for Coastal Biogeochemistry Research, Southern Cross University, Lismore, Australia

³Aix-Marseille Université Université de Toulon, CNRS/INSU, IRD, MIO, UM 110, 13288, Marseille, CEDEX 09, France

⁴Sorbonne Universités (UPMC, Univ Paris 06)-CNRS-IRD-MNHN, LOCEAN Laboratory, 4 place Jussieu, 75005 Paris, France

⁵Department of Oceanography, COPAS SurAustral program and Interdisciplinary Center for Aquaculture Research (INCAR), University of Concepción, Chile

⁶Program of Oceanography, University of Antioquia, Medellín, Columbia

⁷Program of Biology, University of Magdalena, Santa Marta, Columbia

⁸Sorbonne Universités, UPMC Université Paris 06, UMR 7621, Laboratoire d’Océanographie Microbienne, Observatoire Océanologique, 66650 Banyuls/mer, France

Title Page

Abstract

Introduction

Conclusions

References

Tables

Figures



Back

Close

Full Screen / Esc

Printer-friendly Version

Interactive Discussion



Received: 22 November 2014 – Accepted: 25 November 2014 – Published:
19 December 2014

Correspondence to: A. J. Cavagna (acavagna@vub.ac.be)

Published by Copernicus Publications on behalf of the European Geosciences Union.

BGD

11, 18073–18104, 2014

**Biological
productivity regime
and associated N
cycling**

A. J. Cavagna et al.

Title Page

Abstract

Introduction

Conclusions

References

Tables

Figures



Back

Close

Full Screen / Esc

Printer-friendly Version

Interactive Discussion



Abstract

Although the Southern Ocean is considered a High Nutrient Low Chlorophyll area (HNLC), massive and recurrent blooms are observed over and downstream the Kerguelen Plateau. This mosaic of blooms is triggered by a higher iron supply resulting from the interaction between the Antarctic Circumpolar Current and the local bathymetry. Net primary production, N-uptake (NO_3^- and NH_4^+), and nitrification rates were measured at 8 stations in austral spring 2011 (October–November) during the KEOPS2 cruise in the Kerguelen area. Iron fertilization stimulates primary production, with integrated net primary production and growth rates much higher in the fertilized areas (up to $315 \text{ mmol C m}^{-2} \text{ d}^{-1}$ and up to 0.31 d^{-1} , respectively) compared to the HNLC reference site ($12 \text{ mmol C m}^{-2} \text{ d}^{-1}$ and 0.06 d^{-1} , respectively). Primary production is mainly sustained by nitrate uptake, with f ratio (corresponding to NO_3^- uptake / (NO_3^- uptake + NH_4^+ uptake)) lying in the upper end of the observations for the Southern Ocean (up to 0.9). Unexpectedly, we report unprecedented rates of nitrification (up to $\sim 3 \text{ mmol C m}^{-2} \text{ d}^{-1}$, with $\sim 90\%$ of them $< 1 \text{ mmol C m}^{-2} \text{ d}^{-1}$). It appears that nitrate is assimilated in the upper part of the mixed layer (coinciding with the euphotic layer) and regenerated in the lower parts. We suggest that such high contribution of nitrification to nitrate assimilation is driven by (i) a deep mixed layer, extending well below the euphotic layer, allowing nitrifiers to compete with phytoplankton for the assimilation of ammonium, (ii) extremely high rates of primary production for the Southern Ocean, stimulating the release of dissolved organic matter, and (iii) an efficient food web, allowing the reprocessing of organic N and the retention of nitrogen into the dissolved phase through ammonium, the substrate for nitrification.

Biological productivity regime and associated N cycling

A. J. Cavagna et al.

Title Page

Abstract

Introduction

Conclusions

References

Tables

Figures



Back

Close

Full Screen / Esc

Printer-friendly Version

Interactive Discussion



1 Introduction

The Southern Ocean is considered a High Nutrient Low Chlorophyll (HNLC) system due to a combination of several factors, including upwelling of nutrient-rich waters south of the Antarctic Polar Front and, iron (Fe) and light co-limitation for phytoplankton growth (Martin, 1990; Falkowski et al., 1998; Sarmiento et al., 2004). The Southern Ocean is also recognized as a major hot spot for gas exchanges accounting for up to 20 % of the global ocean CO₂ uptake (Takahashi et al., 2009). The concern regarding ongoing climate change has triggered a great interest for this part of the global ocean (Le Quéré et al., 2007).

Since the Iron Hypothesis highlighted by Martin (1990) the last two decades have witnessed an exponential research interest on iron availability and associated biological processes. The aim was to explore the role of iron in enhancing the biological pump and the subsequent increase in the drawdown of atmospheric CO₂. Numerous on-site artificial Fe-enrichment experiments (see Boyd et al., 2007) were conducted in situ to explore the fertilization effect of iron (de Baar et al., 2005, 2008; Boyd et al., 2007; Smetacek et al., 2012; Quéguiner, 2013). In parallel, several naturally Fe-enriched sites were studied (e.g., Boyd et al., 2007) to understand the mechanisms driving such iron fertilization and their impacts on biogeochemical systems without external forcing, i.e. without artificial Fe-enrichment (Blain et al., 2007, 2008; Pollard et al., 2007, 2009; Bowie et al., 2011). The KEOPS project, carried out in the Kerguelen area, is dedicated to the understanding of the functioning of a naturally iron-fertilized system over a large and seasonal scale. For that purpose a first cruise was completed during austral summer 2005 (KEOPS1, February–March; Blain et al., 2007) and a second cruise was completed during austral spring 2011 (KEOPS2, October–November 2011).

Through its crustal and seawater interface, the Kerguelen area (composed of Kerguelen Island, the Kerguelen Plateau and Heard Island in the south-east) enriches the surrounding waters with macronutrients and trace elements. It also strongly impacts the local oceanic physical dynamics due to its Island Mass Effect (IME; Doty and

BGD

11, 18073–18104, 2014

Biological productivity regime and associated N cycling

A. J. Cavagna et al.

Title Page

Abstract

Introduction

Conclusions

References

Tables

Figures

⏪

⏩

◀

▶

Back

Close

Full Screen / Esc

Printer-friendly Version

Interactive Discussion



Biological productivity regime and associated N cycling

A. J. Cavagna et al.

Title Page

Abstract

Introduction

Conclusions

References

Tables

Figures



Back

Close

Full Screen / Esc

Printer-friendly Version

Interactive Discussion



Oguri, 1956). The interactions between geostrophic water flow disturbances due to the presence of the island, the tidal activity over the plateau, and the strong winds characterizing the area produce a complex hydrodynamical environment, resulting from the generation of internal waves, eddies, jets, and Ekman pumping (Heywood et al., 1990; Park et al., 2008; Gille et al., 2014). These characteristics are key factors inducing the fertilization and the associated higher productivities around the Kerguelen Island area as compared to the HNLC surrounding waters (Blain et al., 2001, 2007; Fig. 1). Moreover, a third condition impacting productivity is the proximity of the Polar Front (PF), which trajectory is steered by the bottom topography (Park et al., 2014). Such frontal system by itself offers peculiar conditions inducing significant biological activity (de Baar et al., 1995).

Here we report net primary production at 8 stations visited during KEOPS2, representing the variability encountered over the Kerguelen plateau area and downstream, together with N-uptake (NO_3^- and NH_4^+) and nitrification rates. Regarding the nitrogen cycle, studies conducted during KEOPS1 showed a decoupling of the seasonal use of nitrate and silicic acid stocks over the Kerguelen Plateau (Mosseri et al., 2008), although Si : NO_3 assimilation ratios were close to 1, in accordance with what is expected for non-limiting iron conditions (Takeda, 1998; Hutchins and Bruland, 1998). Mosseri et al. (2008) attributed this peculiar decoupling to the capacity of diatoms to grow on an ammonium stock resulting from a high heterotrophic activity at the end of the productive period, thus highlighting the importance of nitrogen recycling in the surface layer. In this context, the objectives of the studies undertaken during KEOPS2 were:

1. to evaluate and compare the C- and N-assimilation rates during austral spring over the Kerguelen Plateau, in the wake of Kerguelen Island, and at a reference HNLC site,
2. to assess the importance of recycling processes in the supply of phytoplankton nitrogen in the surface layer,
3. to test the intensity of nitrification and its role in the recycling of nitrogen.

2 Materials and methods

The KEOPS 2 expedition took place in the Indian sector of the Southern Ocean during the early spring of 2011 (September to November) on board R/V *Marion Dufresne*. We sampled 8 sites for process studies (Fig. 1), including a reference station (R2) in a HNLC off-plateau region located south-west of Kerguelen Islands; 3 stations within the phytoplankton plume (A3-2, above the Plateau; E4W on the Plateau margin and F-L north of the Polar Front to the east of Kerguelen; and 4 stations (E1, E3, E4E, E5) in a complex recirculation system of a stationary meander confined by the Polar Front.

At these 8 sites we performed isotopic-tracer incubations (24 h) to assess the following rates:

- C-fixation rates (hereafter defined as net primary production) by adding ^{13}C -DIC into incubation bottle, and subsequent measurement of the incorporation of ^{13}C into biomass.
- Ammonium and nitrate uptake rates by adding either $^{15}\text{N-NH}_4^+$ or $^{15}\text{N-NO}_3^-$ into incubation bottle and subsequent measurement of the incorporation of ^{15}N into biomass.
- Nitrification rates by adding $^{15}\text{N-NO}_3^-$ into incubation bottle, the ^{14}N isotopic dilution of nitrate by the oxidation of both ammonium and nitrite by nitrifiers is measured.

The surface water was sampled at 7 to 8 depths corresponding to 75, 45, 25, 16, 4, 1, 0,3, 0,01 % of the surface photosynthetically active radiation (PAR), using Niskin bottles mounted on a rosette fitted with a PAR sensor. For each light level, two acid-cleaned 1 L polycarbonate incubation bottles were filled with seawater. The two bottles were spiked with $200 \mu\text{mol L}^{-1}$ of $^{13}\text{C-HCO}_3^-$ (99 atom ^{13}C %), corresponding to a tracer addition equivalent to $\approx 10\%$ of the surface seawater DIC concentration ($\approx 2 \text{ mM}$), and providing a duplicate of net primary production. One of the bottles was spiked with $^{15}\text{N-NO}_3^-$ and the other with $^{15}\text{N-NH}_4^+$ (98 atom ^{15}N %). The amount of spike added was

18078

BGD

11, 18073–18104, 2014

Biological productivity regime and associated N cycling

A. J. Cavagna et al.

Title Page

Abstract

Introduction

Conclusions

References

Tables

Figures

◀

▶

◀

▶

Back

Close

Full Screen / Esc

Printer-friendly Version

Interactive Discussion



Biological productivity regime and associated N cycling

A. J. Cavagna et al.

Title Page

Abstract

Introduction

Conclusions

References

Tables

Figures

◀

▶

◀

▶

Back

Close

Full Screen / Esc

Printer-friendly Version

Interactive Discussion

calculated taking into account the original nitrate and ammonium concentrations in order to achieve concentration increments $< 10\%$. Incubation bottles were then placed into on-deck incubators, cooled with circulating surface seawater, and wrapped in neutral density screens simulating the photometric depths. Incubation experiments were stopped after 24 h. This relatively long incubation time implies that we probably underestimated uptake rates in case of Eq. (1) release of ^{15}N and ^{13}C to the dissolved organic pool during the course of the experiment (Bronk et al., 1994; Laws et al., 2002) and Eq. (2) ammonification, which would result in diluting the ^{15}N -spiked ammonium pool with ^{14}N . However, the choice of long incubation times was expected to increase sensitivity in order to detect nitrification, and to enable the comparison with Si uptake and dissolution experiments (Closset et al., 2014) carried out over similar 24 h periods.

Both at the initial and final incubation times, subsamples for nitrate (10 mL) and ammonium (2×20 mL) were directly measured with continuous flow analysis (Aminot and K erouel, 2007) and the fluorometric method (Holmes et al., 1999), respectively. A further additional 10 mL was sampled from the $^{15}\text{N}\text{-NO}_3^-$ bottle, filtered using 0.2 μm Acrodisc filters (Sartorius) and stored at -20°C , for later nitrate isotope analysis. The remaining seawater was filtered on pre-combusted (450°C) glass fiber filters (Sartorius, MGF, nominal porosity 0.7 μm , 25 mm diameter). Filters were placed in pre-combusted scintillation vials, dried at 50°C and stored in the dark at room temperature until further analysis at the laboratory.

Particulate organic nitrogen (PON) and particulate organic carbon (POC) concentrations along with their ^{15}N and ^{13}C abundances (atom ^{13}C and ^{15}N %) were analysed via an elemental analyser-isotope ratio mass spectrometer (EA-IRMS) using the method described in Savoye et al. (2004). Atom ^{15}N % for nitrate was measured using the denitrifier method (Sigman et al., 2001) on the 10 mL sub-sampling in the $^{15}\text{N}\text{-NO}_3^-$ bottle. This sample was thawed in the laboratory and 20–30 nmol of nitrate were quantitatively converted to N_2O gas by denitrifying bacteria that lack an active N_2O reductase. The ^{15}N abundance of the N_2O is measured by gas chromatography/isotope ratio mass spectrometry (GC/IRMS) with on-line cryo-trapping.

C-assimilation and ammonium uptake rates (ρNH_4^+) were estimated from the equations of Dugdale and Goering (1967), the following is for C-fixation:

$$V = \frac{(\text{atom}\% \text{ } ^{13}\text{C}_{\text{POC tf}})}{\text{time} \cdot (\text{atom}\% \text{ } ^{13}\text{C}_{\text{DIC ti}})} \quad (1)$$

$$\text{NPP} = [\text{POC}_{\text{tf}}] \cdot V \quad (2)$$

5 where V is the specific C assimilation rate (in d^{-1}), NPP net primary production (in $\mu\text{mol CL}^{-1} \text{d}^{-1}$), $\text{atom}\% \text{ } ^{13}\text{C}$ the measured abundances minus the natural abundances, and tf and ti refer to the final and initial time of incubation, respectively. Except for nitrate for which initial abundances were measured, the initial abundances for both DIC and NH_4^+ were calculated by taking into account the spike addition and isotopic abundance.

10 The nitrate uptake rate (ρNO_3^-) was corrected for the isotope dilution effect during incubation and assessed with the equation provided by Nelson and Goering (1977a, b):

$$V \text{NO}_3^- = \frac{\text{atom}\% \text{ } ^{15}\text{N}_{\text{PON tf}}}{\text{time} \cdot \sqrt{\text{atom}\% \text{ } ^{15}\text{NO}_3^-_{\text{ti}} \cdot \text{atom}\% \text{ } ^{15}\text{NO}_3^-_{\text{tf}}}}$$

$$\rho\text{NO}_3^- = [\text{PON}_{\text{tf}}] \cdot V \text{NO}_3^-$$

15 The nitrification (RNO_3^-) rate was assessed using the integrated rate equation of the Blackburn model (Blackburn, 1979; Elskens et al., 2005):

$$\text{RNO}_3^- = \frac{\ln\left(\frac{\text{atom}\% \text{ } ^{15}\text{NO}_3^-_{\text{ti}}}{\text{atom}\% \text{ } ^{15}\text{NO}_3^-_{\text{tf}}}\right) \cdot [\text{NO}_3^-_{\text{tf}} - \text{NO}_3^-_{\text{ti}}]}{\text{time} \cdot ([\text{NO}_3^-_{\text{tf}}]/[\text{NO}_3^-_{\text{ti}}])}$$

20 Uncertainty on uptake (NPP, ρNH_4 and ρNO_3) and nitrification (RNO_3) rates were assessed using Monte-Carlo simulations assuming normal distribution for all the measured variables.

**Biological
productivity regime
and associated N
cycling**

A. J. Cavagna et al.

[Title Page](#)[Abstract](#)[Introduction](#)[Conclusions](#)[References](#)[Tables](#)[Figures](#)[⏪](#)[⏩](#)[◀](#)[▶](#)[Back](#)[Close](#)[Full Screen / Esc](#)[Printer-friendly Version](#)[Interactive Discussion](#)

The modelled calculated nitrification rates were screened for consistency with observed evolutions of nitrate concentrations over the duration of the incubation experiment and with measured nitrate uptake rates. The difference between nitrate uptake and nitrification should be compatible with the change in nitrate concentration over the duration of the experiment, taking into account a 10 % precision (relative SD) on rates and concentrations measurements. When the rates given by the model were incompatible with concentration evolution, it was considered as an outlier and discarded from the dataset. We point out that measuring nitrification rates under conditions of high ambient nitrate is methodologically challenging. Indeed high nitrate concentration implies (i) a poor sensitivity, which we estimate at $0.26 \mu\text{mol L}^{-1} \text{d}^{-1}$ by taking into account how much nitrification is needed to change the isotopic composition of the nitrate pool by 2sd, and (ii) a poor precision ($\pm 0.26 \mu\text{mol L}^{-1} \text{d}^{-1}$; estimated by taking into account the precision on the isotopic measurement; 2sd). Such values for sensitivity and precision of the nitrification rates exceed most of the nitrification rates reported to date for the open ocean (Ward, 2007).

3 Results

Except for the station (F-L) north of the Polar Front, the different water masses and associated biogeochemical properties were characteristic of the Antarctic Zone: a relatively warmer mixed layer at the surface and the remnant of the winter mixed layer in subsurface (temperature minimum layer; Park et al., 2008). South of the Polar Front, macro-nutrients (PO_4^{3-} , NO_3^- , $\text{Si}(\text{OH})_4$) were present at high and relatively uniform concentrations between stations (Christaki et al., 2014; Closset et al., 2014), with average nitrate concentration of $\sim 25 \mu\text{mol L}^{-1}$ in the mixed layer. In agreement with a progressive nutrient consumption along the meridional water transfer across the Antarctic Circumpolar Current (Sigman et al., 1999; Sarmiento et al., 2004), the station north of the Polar Front (F-L) presented higher surface temperatures (with an increase of $\sim 1\text{--}2^\circ\text{C}$) and lower nitrate concentrations ($\sim 15\text{--}20 \mu\text{mol L}^{-1}$). A slight NH_4^+ and NO_2^- accumu-

lation was observed in the mixed layer all across the study area, but concentrations remained lower than $0.5 \mu\text{mol L}^{-1}$ for both NH_4^+ and NO_2^- (Christaki et al., 2014).

Both particulate organic C and N concentrations (POC and PON) increased from the HNLC reference station (R2) to the meander stations (E stations), and then to the bloom station, over the Kerguelen Southeast Plateau and at the margin (A3-2, E4W) and North of the Polar Front (F-L) (Fig. 2). The high concentrations observed at station E4W are due to the interaction between the meander zone and the plateau at the margin as shown by Lasbleiz et al. (2014). Overall, this spatial distribution of phytoplankton biomass is in agreement with satellite chl *a* observations (Fig. 1).

A positive relationship is apparent between biomass ($\mu\text{mol L}^{-1}$) and assimilation rates ($\mu\text{mol L}^{-1} \text{d}^{-1}$), both for carbon and nitrogen (Fig. 2). Such relationship also holds between biomass and specific uptake rate (V ; d^{-1} ; growth rate) and doubling time ($T_d = \ln(2)/V$; in days). The bloom over the Kerguelen Plateau (A3-2 and E4W) and north of the Polar Front (F-L) presented higher assimilation rates per unit of biomass ($\mu\text{mol C}$ and NL^{-1}) than the stations in the HNLC area (R2) and in the meander (E stations).

In general, vertical profiles of net primary production followed light availability in the mixed layer, with a sharp decrease below the euphotic layer depth (Z_e ; 1% surface PAR depth) (Fig. 3). The primary production activity occurs well below Z_e , although at much lower rates than in the upper levels of the surface layer. This is particularly obvious for the most productive stations; primary production rates are still 0.36, 0.37, and $0.12 \mu\text{mol CL}^{-1}$ at the 0.3% surface PAR level, as compared to rates of 11.9, 8.3, and $6.2 \mu\text{mol CL}^{-1}$ at the surface, respectively at stations PF, E4W, and A3-2. At the 0.01% surface PAR levels values of primary production are close to 0 for the least productive sites but are still significant at PF, E4W, and A3-2 stations (respectively 0.12, 0.06, and $0.08 \mu\text{mol CL}^{-1}$).

Vertical profiles of N-assimilation rates closely paralleled the vertical evolution of primary production, for both NO_3^- and NH_4^+ uptake. The decrease in NH_4^+ assimilation rates with depth was less severe than that for NO_3^- . Assimilation of nitrate is more en-

BGD

11, 18073–18104, 2014

**Biological
productivity regime
and associated N
cycling**

A. J. Cavagna et al.

Title Page

Abstract

Introduction

Conclusions

References

Tables

Figures

◀

▶

◀

▶

Back

Close

Full Screen / Esc

Printer-friendly Version

Interactive Discussion



ergetically demanding than ammonium, because nitrate has to be first reduced into ammonium, an ATP demanding processes (Mulholland and Lomas, 2007). In most of the stations, nitrate was still preferentially assimilated over ammonium (Fig. 4a), resulting in high f ratio defined as NO_3^- uptake / (NO_3^- uptake + NH_4^+ uptake) ratio according to Dugdale and Goering (1967). The f ratios in the euphotic layer increased with N-uptake rates ($\text{NO}_3^- + \text{NH}_4^+$), from ~ 0.4 in the less productive HNLC reference station to ~ 0.9 north of the Polar Front.

Unexpectedly, some nitrification rates were significant in the mixed layer, reaching values up to $\sim 3 \mu\text{mol L}^{-1} \text{d}^{-1}$, with $\sim 90\%$ of the data falling below $1 \mu\text{mol L}^{-1} \text{d}^{-1}$ (Fig. 3). In general, nitrification rates reached maxima near the bottom of the euphotic layer (Fig. 3).

4 Discussion

4.1 High primary production in naturally iron-fertilized blooms

At the most productive stations of the different blooms, primary production still persists, but a much lower rates, at levels far deeper than the 1 % surface PAR depth, traditionally regarded as the lower limit of the euphotic layer. Such an observation is not unusual and this has been recently discussed by Marra et al. (2014).

For this reason, we have calculated the vertically-integrated primary production rates are calculated from the surface down to the mixed layer depth. The spring phytoplankton blooms developing over and downstream the Kerguelen Southeast Plateau exhibit very high rates of net primary production (up to $315 \text{ mmol C m}^{-2} \text{d}^{-1}$;) as compared to the adjacent HNLC area ($\sim 13 \text{ mmol C m}^{-2}$) (Fig. 5). Our value of primary production at the HNLC station falls within the range of values reported for such environments. It is in the same order of magnitude as the value of $\sim 20 \text{ mmol C m}^{-2}$ reported for the HNLC reference site of CROZEX in austral spring by Seeyave et al. (2007). In the Pacific sector of the Southern Ocean, Hiscock et al. (2003) report values ranging between 13

BGD

11, 18073–18104, 2014

Biological productivity regime and associated N cycling

A. J. Cavagna et al.

Title Page

Abstract

Introduction

Conclusions

References

Tables

Figures

◀

▶

◀

▶

Back

Close

Full Screen / Esc

Printer-friendly Version

Interactive Discussion



to $93 \text{ mmol C m}^{-2} \text{ d}^{-1}$ all over the seasonal cycle in an area extending from 54 to 72° S spanning the Sub-Antarctic Zone, the Polar Frontal Zone, to the ice-edge in the wake of the retreating sea-ice. For the Atlantic sector, such low primary production rates, down to 25 mmol C m^{-2} are also reported by Jochem et al. (1995) in the Permanently Open Ocean Zone, south of the Polar Front, during austral spring. Finally, at a broader spatial scale, Arrigo et al. (2008) give values ranging from $4\text{--}6 \text{ mmol C m}^{-2}$ in winter to $25\text{--}33 \text{ mmol C m}^{-2}$ at the peak of the spring bloom in their so-called pelagic zone of the Southern Ocean.

Several massive blooms occur in the core of the Antarctic Circumpolar Current (Fig. 1): (i) over the Kerguelen Southeast Plateau, remarkably constrained by the bathymetry, (ii) in a plume extending eastward through the interaction between the Polar Front jet, crossing the plateau in a narrow mid-depth channel just to the south of the Kerguelen Island, and the rise bordering the basin to the north, (iii) to the easternmost part of the study area in a zone of retroflexion of the Polar Front and of eddy mixing between Antarctic and Sub-Antarctic Surface Waters (see Park et al., 2014). This complex distribution is in agreement with an input of iron from the interaction between the iron-deficient Antarctic Circumpolar Current and the local bathymetry (Blain et al., 2007; Sokolov and Rintoul, 2007). Trace metals, and iron in particular, are required for many important cellular processes such as photosynthesis (including photo-adaptation), respiration, and nitrate reduction. Iron-enrichment experiments ranging from bottle incubations to large scale open-ocean amendment studies have demonstrated that iron supply stimulates phytoplankton growth in the Southern Ocean (Martin, 1990; de Baar et al., 1990, 2005; Boyd et al., 2007). Primary production up to $< 130 \text{ mmol C m}^{-2} \text{ d}^{-1}$ has been reported in these iron-fertilized patches (Gall et al., 2001; Gervais et al., 2002; Coale et al., 2004; Smetacek et al., 2012). Naturally iron fertilized systems usually present higher rates of primary production, similar to the KEOPS study: e.g., up to $\sim 275 \text{ mmol C m}^{-2} \text{ d}^{-1}$ over the South Georgia plateau (Korb et al., 2005); and up to $\sim 250 \text{ mmol C m}^{-2} \text{ d}^{-1}$ within the fast-flowing, iron-rich jet of the Polar Front in the Atlantic sector (Jochem et al., 1995) and in the iron-fertilized plume

BGD

11, 18073–18104, 2014

**Biological
productivity regime
and associated N
cycling**

A. J. Cavagna et al.

Title Page

Abstract

Introduction

Conclusions

References

Tables

Figures

⏪

⏩

◀

▶

Back

Close

Full Screen / Esc

Printer-friendly Version

Interactive Discussion



described enrichment over the plateau and the spreading of this enrichment eastward through the additional interaction between the Polar Front jet and local bathymetry (Mongin et al., 2008; Sanial et al., 2014). This mode of supply can be compared with the Polar Front associated bloom in the Atlantic sector, where iron is supplied by lateral advection from the Patagonian shelves and islands in the Scotia Ridge area (de Baar et al., 1995) or by direct lithogenic aerosol deposits (Quéguiner et al., 1997). Similar increases in growth rate driven by the degree of iron fertilization (Fig. 2) have been reported earlier for the Southern Ocean (e.g., the growth rate increase from < 0.1 to 0.5 d^{-1} in the SOIREE fertilized patch; Gall et al., 2001).

Net primary production over the Kerguelen Plateau measured during summer (January–February, KEOPS 1; Mosseri et al., 2008), reached values close to $\sim 80 \text{ mmol C m}^{-2} \text{ d}^{-1}$. This was lower than the estimates for spring in the present study ($\sim 200 \text{ mmol C m}^{-2} \text{ d}^{-1}$) (Fig. 5). Such seasonal pattern is in agreement with the seasonal evolution observed from satellite chl *a* observations. These show that the bloom starts in early November, reaches its maximum level in late November–Early December, and collapses in January–February (Mongin et al., 2008; Blain et al., 2013). Contrasting with the spring situation studied in the present study, in summer there is no relationship between biomass and primary production or growth rate (Fig. 6). In early February, primary production and growth rate decreased rapidly from about 14 down to $2 \mu\text{mol CL}^{-1} \text{ d}^{-1}$, and from ~ 0.3 down to 0.01 d^{-1} , respectively. Associated with these changes, the mixed layer evolved from an autotrophic system, typical for spring, to a heterotrophic situation where respiration exceeds photosynthesis (Lefèvre et al., 2008; Christaki et al., 2014). With still nitrate and phosphate at non-limiting concentration, a top-down control of the mortality of phytoplankton cells (mostly diatoms; George et al., 2014; Sackett et al., 2014) is the most likely cause of this change (Carlotti et al., 2008; Brussard et al., 2008; Sarthou et al., 2008). Late summer Si limitation of diatom growth cannot be ruled out too, since measured silicic acid concentrations ($\sim 1 \mu\text{mol L}^{-1}$) are significantly below measured half saturation constants for Si-uptake ($5\text{--}15 \mu\text{mol L}^{-1}$; Mosseri et al., 2008). However, Fv/Fm ratios over the

Biological productivity regime and associated N cycling

A. J. Cavagna et al.

[Title Page](#)[Abstract](#)[Introduction](#)[Conclusions](#)[References](#)[Tables](#)[Figures](#)[◀](#)[▶](#)[◀](#)[▶](#)[Back](#)[Close](#)[Full Screen / Esc](#)[Printer-friendly Version](#)[Interactive Discussion](#)

plateau remained high indicating the phytoplankton community was relieved from nutrient stress, including iron (Timmermans et al., 2008).

To conclude, the resulting increase in integrated primary production (up to 8 times; Fig. 5) between fertilized (Plateau and Polar Front) and unfertilized areas (HNLC reference site) is similar to the largest increase reported for artificial iron addition experiments worldwide (Boyd et al., 2007; up to 10 times). Despite the much higher primary production for the fertilized area in comparison with the HNLC area, the export of organic matter remains relatively small during spring and summer (Savoye et al., 2008; Planchon et al., 2014). Low export efficiency suggests that the products of primary production are mainly recycled within the mixed layer by an efficient microbial loop (Sarhou et al., 2008; Obernosterer et al., 2008; Christaki et al., 2014; Malit et al., 2014). The carbon sequestration efficiency induced by iron-fertilization remains, therefore, relatively low (Blain et al., 2007, 2014b).

4.2 Upper Ocean N cycling: high nitrification rates in deep productive mixed layer

Except for the HNLC reference station, nitrate uptake was higher than ammonium uptake in the euphotic layer (Fig. 4a). The f ratio increases with measured N-uptake rates ($\text{NO}_3^- + \text{NH}_4^+$), from ~ 0.4 in the less productive HNLC reference station to ~ 0.9 north of the Polar Front. The latter value lies in the upper end for the Southern Ocean, and is indicative of a nearly complete NO_3^- -based primary production (Savoye et al., 2004; and references therein). Below the euphotic layer, ammonium is preferentially assimilated over nitrate, with f ratios ranging between 0.1 and 0.5 (not shown). Assimilation of nitrate is more energetically demanding than ammonium and should be more dependent on light. Once nitrate has been transported into the cell, it has to be further reduced into ammonium before it gets assimilated (Mulholland and Lomas, 2007). At the end of summer, the f ratio over the plateau decreases rapidly, from 0.6 to 0.2, indicating that the system evolved from a nitrate-based to an ammonium-based primary production (Mosseri et al., 2008; P. Raimbault, unpub. results 2014). Such evolution

Biological productivity regime and associated N cycling

A. J. Cavagna et al.

Title Page

Abstract

Introduction

Conclusions

References

Tables

Figures

◀

▶

◀

▶

Back

Close

Full Screen / Esc

Printer-friendly Version

Interactive Discussion



**Biological
productivity regime
and associated N
cycling**

A. J. Cavagna et al.

[Title Page](#)[Abstract](#)[Introduction](#)[Conclusions](#)[References](#)[Tables](#)[Figures](#)[Back](#)[Close](#)[Full Screen / Esc](#)[Printer-friendly Version](#)[Interactive Discussion](#)

is in agreement with an increase in ammonium availability in a decaying bloom. We acknowledge that f ratios can be overestimated, since it is likely that also organic nitrogen compounds are incorporated by phytoplankton (Bronk et al., 2007). However, we note that urea uptake, a proxy for dissolved organic N assimilation, is usually relatively low south of the Polar Front, where dissolved inorganic N is abundant (Waldron et al., 1995; Sambrotto et al., 2000; Savoye et al., 2004).

Except for the HNLC reference station, the euphotic layer depth is relatively constant between stations while mixed layer depth varies significantly. The latter is generally deeper, more variable and extends more significantly below the euphotic layer over the Kerguelen plateau and at the HNLC reference station. Such spatial segregation of light distribution in the mixed layer, more or less expressed between stations, has profound consequences on the cycling of nitrogen. Nitrification rates are high (up to $3 \mu\text{mol L}^{-1} \text{d}^{-1}$, but $\sim 90\%$ of them $< 1 \mu\text{mol L}^{-1} \text{d}^{-1}$) at low light intensities, and insignificant (below our detection limit) at high light intensities (Fig. 4b). Such a distribution fits supports the fact that nitrification is known to be inhibited by light (Hagopian and Riley, 1998; Ward, 2007) even though if in a recent compilation, Yool et al. (2007) observed no clear relationship in the euphotic layer with depth. The review of Ward (2007) shows that highest nitrification rates occur near the bottom of the euphotic layer. At this depth light intensity is reduced, phytoplankton is light limited (Fig. 2), and nitrifiers can compete with phytoplankton for ammonium. Indeed, the energy yield of ammonium oxidation is low (Hagopian and Riley, 1998) and in case there is enough light to sustain primary productivity and associated nutrient-assimilation, nitrifiers are unlikely to out-compete phytoplankton.

In the mixed layer the extinction of light with depth promotes nitrate assimilation in the upper parts (euphotic layer) and nitrification in the lower parts (Figs. 2 and 4b). Since a deep mixed layer is a common feature in the Southern Ocean, iron fertilization should boost nitrification by stimulating the release of dissolved organic matter in this area, originated by higher phytoplankton growth (Malits et al., 2014). In turn the microbial foodweb is stimulated and will thus process organic matter more efficiently

Biological productivity regime and associated N cycling

A. J. Cavagna et al.

Title Page

Abstract

Introduction

Conclusions

References

Tables

Figures

◀

▶

◀

▶

Back

Close

Full Screen / Esc

Printer-friendly Version

Interactive Discussion



(Obernosterer et al., 2008; Christaki et al., 2014; Malits et al., 2014). The effect of viruses is also enhanced (Malits et al., 2014), increasing bacterial mortality and allowing the retention of organic matter within the mixed layer. These conditions combined with grazing (Brussard et al., 2008; Sarthou et al., 2008) likely promote the release of ammonium from remineralization of organic N and excretion by zooplankton. Ammonium is the substrate for nitrification and larger substrate availability will likely be favorable for the development of an efficient nitrifier community.

In this study, the nitrification rates are well above the maximum rates reported for the open ocean, up to $0.75 \mu\text{mol L}^{-1} \text{d}^{-1}$ in the Peru Upwelling (Lipschultz et al., 1991; Ward, 2007), and for the Southern Ocean ($< 0.1 \mu\text{mol L}^{-1} \text{d}^{-1}$; Olson, 1981; Bianchi et al., 1997). The available Southern Ocean nitrification data pertains to fall and winter, seasons during which primary production and remineralization are expected to be low. Such high nitrification rates are likely to be driven by: (i) very high rates of primary production (Sect. 4.1), similar to the most productive areas in the ocean; (ii) the indirect iron-driven effect on the ability of the microbial foodweb to process organic matter (Malits et al., 2014; Christaki et al., 2014); and (iii) a shallower euphotic layer compared to the mixed layer, allowing nitrifiers to compete with phytoplankton for the assimilation of ammonium in the depth interval between the bottom of the euphotic layer and the mixed layer. This is further confirmed by Fripiat et al. (in prep) who simulated, over the Kerguelen Plateau, the change from October to February in the concentration of the fixed N pools and their isotopic composition ($\delta^{15}\text{N}$ and $\delta^{18}\text{O}$), and show that nitrification can contribute between 40 and 80 % to the seasonal nitrate assimilation. Such findings have profound consequences on the concept of new production (Dudgale and Goering, 1967; Eppley and Petterson, 1979). New production is functioning on the supply of what it is called “new nutrients”. New nutrients are distantly produced, supplied into the mixed layer by vertical mixing (both in winter and in summer), and assimilated during the vegetative season. To balance this supply, new production has to be equal to the production exported to depth, stripping out nutrients from the mixed layer. Especially in the Southern Ocean, with the ventilation of nutrient-rich deep waters, nitrate is gener-

**Biological
productivity regime
and associated N
cycling**

A. J. Cavagna et al.

[Title Page](#)[Abstract](#)[Introduction](#)[Conclusions](#)[References](#)[Tables](#)[Figures](#)[◀](#)[▶](#)[◀](#)[▶](#)[Back](#)[Close](#)[Full Screen / Esc](#)[Printer-friendly Version](#)[Interactive Discussion](#)

ally considered as a new nutrient, with little regeneration in the mixed layer. However, several recent studies highlight that nitrification rates in the surface waters at the global scale has been underestimated (Yool et al., 2007; Ward, 2007; Clark et al., 2008). The Southern Ocean is still generally presented as an exception. Indeed, reported nitrification rates are low (Olson, 1981; Bianchi et al., 1998), but these studies, as described before, are not representative of the bloom condition. Instead, we show that nitrification efficiently regenerates nitrate over and downstream the Kerguelen Plateau. Iron fertilization by the plateau likely promotes higher nitrification rates than in the HNLC area. However, deep mixed layers are widespread in the Southern Ocean. It appears likely that the decoupling between nitrate assimilation and nitrification with depth in the mixed layer, is in some degree an ubiquitous condition during the vegetative season. High mixed layer nitrification is also in agreement with (i) the measured low carbon export efficiency (NPP/²³⁴Th-export; Savoye et al., 2008; Planchon et al., 2014), and (ii) the low nitrate seasonal depletion (Mosseri et al., 2008) despite high nitrate assimilation rates. Significant nitrification can also explain why silicic acid is depleted (with high biogenic silica production/dissolution ratio) but not nitrate (Mosseri et al., 2008; Closset et al., 2014). Si : NO₃ assimilation ratios were close to 1 (Mosseri et al., 2008; Closset et al., 2014), in accordance with what is expected for non-limiting iron conditions (Takeda, 1998; Hutchins and Bruland, 1998). Without nitrification, nitrate will be depleted as silicic acid. The hypothesis puts forward in Mosseri et al. (2008), attributing this peculiar decoupling to the capacity of diatoms to grow on an ammonium stock resulting from a high heterotrophic activity, is unlikely. Ammonium assimilation rates are much lower than nitrate and nitrification efficiently competes with phytoplankton for ammonium.

5 Conclusions

This study further confirms the impact of iron-fertilization on primary production in the Southern Ocean. Fertilized areas present much higher integrated primary production

Biological productivity regime and associated N cycling

A. J. Cavagna et al.

Title Page

Abstract

Introduction

Conclusions

References

Tables

Figures

⏪

⏩

◀

▶

Back

Close

Full Screen / Esc

Printer-friendly Version

Interactive Discussion

(up to $315 \text{ mmol C m}^{-2} \text{ d}^{-1}$) and carbon growth rates (up to 0.31 d^{-1}) than unfertilized HNLC areas ($12 \text{ mmol C m}^{-2} \text{ d}^{-1}$; 0.06 d^{-1} , respectively). Primary production in the euphotic layer of the fertilized areas is mainly sustained by nitrate uptake (f ratio up to 0.9). In the unfertilized areas, the contribution of ammonium to primary production increases, with f ratio down to 0.1.

Unexpectedly, nitrification rates are high (up to $\sim 3 \mu\text{mol L}^{-1} \text{ d}^{-1}$, with $\sim 90\%$ of them $< 1 \mu\text{mol L}^{-1} \text{ d}^{-1}$) and mirrors nitrate uptake rates with depth. Nitrate is mainly assimilated in the upper parts of the deep mixed layer, corresponding to the euphotic layer (between 100 and 1% PAR), and regenerated below. Such high nitrification rates could be explained by (i) deep mixed layer depth, encompassing the euphotic layer, inducing a spatial segregation within the mixed layer of light, (ii) unprecedented rates of primary production, corresponding to one of the most productive place in the open ocean, stimulating the release of dissolved organic matter and secondary primary production, (iii) an efficient microbial foodweb, reprocessing efficiently organic N into ammonium, the substrate of nitrification. These conditions should be favorable for the development of an efficient nitrifier community.

Acknowledgements. Our warm thanks go to the Captain, officers and crew of the R/V *Marion Dufresne* for their support during the KEOPS 2 field work. This research was supported by the Federal Belgian Science Policy Office (BELSPO), Science for Sustainable Development (SSD) program (contract SD/CA/05A); Flanders Research Foundation (FWO grant G071512N); VUB Strategic Research Plan. François Fripiat is a post-doctoral fellow with the Flanders Research Foundation (FWO, Belgium). Camila Fernandez was partially funded by Fondap 15 110 027. LF-L received support from the LIA MORFUN project. KEOPS-2 project was supported by the French Research program of INSU-CNRS LEFE-CYBER (“Les enveloppes fluides et l’environnement” – “Cycles biogéochimiques, environnement et ressources”), the French ANR (“Agence Nationale de la Recherche”, SIMI-6 program), the French CNES (“Centre National d’Etudes Spatiales”) and the French Polar Institute IPEV (Institut Polaire Paul-Emile Victor).

References

- Aminot, A. and K erouel, R.: Dosage Automatique des Nutriments dans les Eaux Marines: Methods en Flux Continu, Ed. Ifremer, 2007.
- Antcibor, I., Eschenbach, A., Zubrzycki, S., Kutzbach, L., Bolshiyarov, D., and Pfeiffer, E.-M.: Trace metal distribution in pristine permafrost-affected soils of the Lena River delta and its hinterland, northern Siberia, Russia, *Biogeosciences*, 11, 1–15, doi:10.5194/bg-11-1-2014, 2014.
- Arrigo, K. R., van Dijken, G. L., and Bushinsky, S.: Primary production in the Southern Ocean, 1997–2006, *J. Geophys. Res.*, 113, C08004, doi:10.1029/2007JC004551, 2008.
- Bianchi, M., Feliatra, F., Tr guer, P., Vincedeau, M.-A., and Morvan, J.: Nitrification rates, ammonium and nitrate distribution in upper layers of the water column and in sediments of the Indian sector of the Southern Ocean, *Deep-Sea Res. Pt. II*, 44, 1017–1032, 1997.
- Blain, S., Tr guer, P., Belviso, S., Bucciarelli, E., Denis, M., Desabre, S., Fiala, M., Jezequel, V. M., Lefevre, J., Mayzaud, M., Marty, J.-C and Razouls, S.: A biogeochemical study of the island mass effect in the context of the iron hypothesis: Kerguelen Islands, Southern Ocean. *Deep-Sea Res. Pt. I*, 48, 163–187, 2001.
- Blain, S., Qu guiner, B., Armand, L., Belviso, S., Bombled, B., Bopp, L., Bowie, A., Brunet, C., Brussaard, C., Carlotti, F., Christaki, U., Corbi re, A., Durand, I., Ebersbach, F., Fuda, J.-L., Garcia, N., Gerringa, L., Griffiths, B., Guigue, C., Guillerm, C., Jacquet, S., Jean-del, C., Laan, P., Lef vre, D., Lo Monaco, C., Malits, A., Mosseri, J., Obernosterer, I., Park, Y.-H., Picheral, M., Pondaven, P., Remenyi, T., Sandroni, V., Sarthou, G., Savoye, N., Scouarnec, L., Souhaut, M., Thuiller, D., Timmermans, K., Trull, T., Uitz, J., van Beek, P., Veldhuis, M., Vincent, D., Viollier, E., Vong, L., and Wagener, T.: Effect of natural iron fertilization on carbon sequestration in the Southern Ocean, *Nature*, 446, 1070–1074, doi:10.1038/nature05700, 2007.
- Blain, S., Qu guiner, B., and Trull, T. W.: The natural iron fertilization experiment KEOPS (Kerguelen Ocean and Plateau compared study): an overview, *Deep-Sea Res. Pt. II*, 55, 559–565, 2008.
- Blain, S., Capparos, J., Gu neugu s, A., Obernosterer, I., and Oriol, L.: Distributions and stoichiometry of dissolved nitrogen and phosphorus in the iron fertilized region near Kerguelen (Southern Ocean), *Biogeosci. Discuss.*, 11, 9949–9977, 2014.

BGD

11, 18073–18104, 2014

Biological productivity regime and associated N cycling

A. J. Cavagna et al.

Title Page

Abstract

Introduction

Conclusions

References

Tables

Figures

◀

▶

◀

▶

Back

Close

Full Screen / Esc

Printer-friendly Version

Interactive Discussion



Biological productivity regime and associated N cycling

A. J. Cavagna et al.

Title Page

Abstract

Introduction

Conclusions

References

Tables

Figures

◀

▶

◀

▶

Back

Close

Full Screen / Esc

Printer-friendly Version

Interactive Discussion



- Bowie, A., Trull, T. W., and Dehairs, F.: Estimating the sensitivity of the subantarctic zone to environmental change: the SAZ-sense project, *Deep-Sea Res. Pt. II*, 58, 2051–2058, 2011.
- Boyd, P. W., Jickells, T., Law, C. S., Blain, S., Boyle, E. A., Buesseler, K. O., Coale, K. H., Cullen, J. J., de Baar, H. J. W., Follows, M., Harvey, M., Lancelot, C., Levasseur, M., Owens, N. P. J., Pollard, R., Rivkin, R. B., Sarmiento, J., Schoemann, V., Smetacek, V., Takeda, S., Tsuda, A., Turner, S., and Watson, A. J.: Mesoscale iron enrichment experiments 1993–2005: synthesis and future directions, *Science*, 315, 612–6117, doi:10.1126/science.1131669, 2007.
- Bronk, D. A., Glibert, P. M., and Ward, B. B.: Nitrogen uptake, dissolved organic nitrogen release, and new production, *Science*, 265, 1843–1846, 1994.
- Bronk, D. A., See, J. H., Bradley, P., and Killberg, L.: DON as a source of bioavailable nitrogen for phytoplankton, *Biogeosciences*, 4, 283–296, doi:10.5194/bg-4-283-2007, 2007.
- Brussaard, C. P. D., Timmermans, K. R., Uitz, J., and Veldhuis, M. J. W.: Virioplankton dynamics and virally induce phytoplankton lysis versus microzooplankton grazing southeast of the Kerguelen (Southern Ocean), *Deep-Sea Res. Pt. II*, 55, 752–765, 2008.
- Carlotti, F., Thibault-Botha, D., Nowaczyk, A., and Lefèvre, D.: Zooplankton community structure, biomass and role in carbon fluxes during the second half of a phytoplankton bloom in the eastern sector of the Kerguelen shelf (January–February 2005), *Deep-Sea Res. Pt. II*, 55, 720–733, 2008.
- Christaki, U., Lefèvre, D., Georges, C., Colombet, J., Catala, P., Courties, C., Sime-Ngando, T., Blain, S., and Obernosterer, I.: Microbial food web dynamics during spring phytoplankton blooms in the naturally iron-fertilized Kerguelen area (Southern Ocean), *Biogeosciences Discuss.*, 11, 6985–7028, doi:10.5194/bgd-11-6985-2014, 2014.
- De Baar, H. J. W., Buma, A. G. J., Nolting, R. F., Cadée, G. C., Jacques, G., and Treguer, P. J.: On iron limitation of the Southern Ocean: experimental observations in the Weddell and Scotia Seas, *Mar. Ecol.-Prog. Ser.*, 65, 105–122, 1990.
- De Baar, H. J. W., de Jong, J. T. M., Bakker, D. C. E., Löscher, B. M., Veth, C., Bathmann, U., and Smetacek, V.: Importance of iron for plankton blooms and carbon dioxide drawdown in the Southern Ocean, *Nature*, 373, 412–415, 1995.
- De Baar, H. J. W., Boyd, P. W., Coale, K. H., Landry, M. R., Tsuda, A., Assmy, P., Bakker, D. C. E., Bozec, Y., Barber, R. T., Brzezinski, M. A., Buesseler, K. O., Boyé, M., Croot, P. L., Gervais, F., Gorbunov, M. Y., Harrison, P. J., Hiscock, W. T., Laan, P., Lancelot, C., Law, C. S., Levasseur, M., Marchetti, A., Millero, F., Nishioka, J., Nojima, Y.,

Biological productivity regime and associated N cycling

A. J. Cavagna et al.

Title Page

Abstract

Introduction

Conclusions

References

Tables

Figures

⏪

⏩

◀

▶

Back

Close

Full Screen / Esc

Printer-friendly Version

Interactive Discussion

van Oijen, T., Riebesell, U., Rijkenberg, M. J. A., Saito, H., Takeda, S., Timmermans, K. R., Veldhuis, M. J. W., Waite, A. M., and Wong, C.-S.: Synthesis of iron fertilization experiments: from the iron age in the age of enlightenment, *J. Geophys. Res.*, 110, C09S16, doi:10.1029/2004JC002601, 2005.

5 Dugdale, R. C. and Goering, J. J.: Uptake of new and regenerated form of nitrogen in primary productivity, *Limnol. Oceanogr.*, 12, 196–206, 1967.

Elskens, M., Baeyens, W., Brion, N. N., De Galan, S., Goeyens, L., and de Brauwere, A.: Reliability of N flux rates estimated from ¹⁵N enrichment and dilution experiments in aquatic systems, *Global Biogeochem. Cy.*, 19, GB4028, doi:10.1029/2004GB002332, 2005.

10 Eppley, R. W.: Temperature and phytoplankton growth in the sea, *Fish. B-NOAA*, 70, 1063–1085, 1972.

Eppley, R. W. and Peterson, B. J.: Particulate organic matter flux and planktonic new production in the deep ocean, *Nature*, 282, 677–680, 1979.

Falkowski, P. G., Barber, R. T., and Smetacek, V.: Biogeochemical controls and feedbacks on ocean primary production, *Science*, 281, 200–206, 1998.

15 Fripiat, F., Elskens, M., Trull, T. W., Blain, S., Cavagna, A.-J., Fernandez, C., Fonseca-Batista, D., Planchon, F., Raimbault, P., Roukaert, A., and Dehairs, F.: Significant mixed layer nitrification in a natural iron-fertilized bloom of the Southern Ocean, *Global Biogeochem. Cy.*, in review, 2014.

20 Gall, M. P., Strzepek, R., Maldonado, M., and Boyd, P.: Phytoplankton processes. Part 2: Rates of primary production and factors controlling algal growth during the Southern Ocean Iron Release Experiment (SOIREE), *Deep-Sea Res. Pt. II*, 48, 2571–2590, 2001.

Gervais, F., Riebesell, U., and Gorbunov, M. Y.: Changes in primary productivity and chlorophyll *a* in response to iron fertilization in the southern polar frontal zone, *Limnol. Oceanogr.*, 47, 1324–1335, 2002.

25 Georges, C., Monchy, S., Genitsaris, S., and Christaki, U.: Protist community composition during early phytoplankton blooms in the naturally iron-fertilized Kerguelen area (Southern Ocean), *Biogeosciences*, 11, 5847–5863, doi:10.5194/bg-11-5847-2014, 2014.

Gille, S. T., Carranza, M. M., Cambra, R., and Morrow, R.: Wind-induced upwelling in the Kerguelen Plateau region, *Biogeosciences*, 11, 6389–6400, doi:10.5194/bg-11-6389-2014, 2014.

30 Hagopian, D. S. and Riley, J. G.: A closer look at the bacteriology of nitrification, *Aquacult. Eng.*, 19, 223–244, 1998.

Hiscock, M. R., Marra, J., Smith Jr., W. O., Goericke, R., Measures, C., Vink, S., Olson, R. J., Sosik, H. M., and Barber, R. T.: Primary productivity and its regulation in the Pacific Sector of the Southern Ocean, *Deep-Sea Res. Pt. II*, 50, 533–558, 2003.

5 Holmes, R. H., Aminot, A., K rouel, R., Hooker, B. A., and Peterson, B. J.: A simple and precise method for measuring ammonium in marine and freshwater ecosystems, *Canadian Fisheries and Aquat. Sci.*, 56, 1801–1808, 1999.

Jacquet, S. H. M., Dehairs, F., Cavagna, A. J. Planchon, F., Monin, L., and Andr  L.: early season mesopelagic carbon remineralization and transfer efficiency in the naturally iron-fertilized Kerguelen area, *Biogeosciences*, this issue, 2014.

10 Korb, R. E., Whitehouse, M. J., Thorpe, S. E., and Gordon, M.: Primary production across the Scotia Sea in relation to the physic-chemical environment, *J. Marine Syst.*, 57, 231–249, 2005.

Laws, E., Sakshaug, E., Babin, M., Dandonneau, Y., Falkowski, P., Geider, R., Legendre, L., Morel, A., Sondergaard, M., Takahashi, M., and Williams, P. J.: Photosynthesis and primary productivity in marine ecosystems: practical aspects and application of techniques, *Joint Global Ocean Flux Study – JGOFS – Report No. 36*, 2002.

15 Le Qu r , C., R denbeck, C., Buithenhuis, E. T., Conway, T. J., Langenfelds, R., Gomez, A., Labuschagne, C., Ramonet, M., Nakazawa, T., Metzl, N., Gillett, N., and Heinmann, M.: Saturation of Southern Ocean CO₂ sink due To recent climate change, *Science*, 316, 1735–1738, doi:10.1126/science.1136188, 2007.

20 Lipschultz, F., Wofsy, S. C., Ward, B. B., Codispoti, L. A., Friedrich, G., and Elkins, J. W.: Bacterial transformations of inorganic nitrogen in the oxygen-deficient waters of the Eastern Tropical South Pacific Ocean, *Deep-Sea Res. Pt. II*, 37, 1513–1541, 1991.

25 Malits, A., Christaki, U., Obernosterer, I., and Weinbauer, M. G.: Enhanced viral production and virus-mediated mortality of bacterioplankton in a natural iron-fertilized bloom above the Kerguelen Plateau, *Biogeosciences Discuss.*, 11, 10827–10862, doi:10.5194/bgd-11-10827-2014, 2014.

Martin, J. H.: Glacial interglacial CO₂ change: the iron hypothesis, *Paleoceanography*, 5, 1–13, 1990.

30 Mongin, M., Molina, E., and Trull, T. W.: Seasonality and scale of the Kerguelen plateau phytoplankton bloom: a remote sensing and modeling analysis of the influence of natural iron fertilization in the Southern Ocean, *Deep-Sea Res. Pt. II*, 55, 880–892, 2008.

Biological productivity regime and associated N cycling

A. J. Cavagna et al.

[Title Page](#)

[Abstract](#)

[Introduction](#)

[Conclusions](#)

[References](#)

[Tables](#)

[Figures](#)



[Back](#)

[Close](#)

[Full Screen / Esc](#)

[Printer-friendly Version](#)

[Interactive Discussion](#)



Biological productivity regime and associated N cycling

A. J. Cavagna et al.

[Title Page](#)

[Abstract](#)

[Introduction](#)

[Conclusions](#)

[References](#)

[Tables](#)

[Figures](#)

[⏪](#)

[⏩](#)

[◀](#)

[▶](#)

[Back](#)

[Close](#)

[Full Screen / Esc](#)

[Printer-friendly Version](#)

[Interactive Discussion](#)



Mosseri, J., Quéguiner, B., Armand, L., and Cornet-Barthaux, V.: Impact of iron on silicon utilization by diatoms in the Southern Ocean: a case study of Si/N cycle decoupling in a naturally iron enriched area, *Deep-Sea Res. Pt. II*, 55, 801–819, 2008.

Obernosterer, I., Christaki, U., Lefèvre, D., Catala, P., Van Wambeke, F., and Lebaron, P.: Rapid bacterial mineralization of organic carbon produced during a phytoplankton bloom induced by natural iron fertilization in the Southern Ocean, *Deep-Sea Res. Pt. II, Topic. Stud. Oceanogr.*, 55, 777–789, 2008.

Olson, R. J.: ^{15}N tracer studies of the primary nitrite maximum, *J. Mar. Res.*, 39, 203–238, 1981.

Park, Y.-H., Roquet, F., Durand, I., and Fuda, J.-L.: Large-scale circulation over and around the Northern Kerguelen Plateau, *Deep-Sea Res. Pt. II*, 55, 566–581, 2008.

Park, Y.-H., Durand, I., Kestenare, E., Rougier, G., Zhou, M., d'Ovidio, F., Cotté, C., and Lee, J. H.: Polar Front around the Kerguelen Islands: an up-to-date determination and associated circulation of surface/subsurface waters, *J. Geophys. Res.*, 119, 6575–6592, 2014.

Planchon, F., Ballas, D., Cavagna, A.-J., Bowie, A. R., Davies, D., Trull, T., Laurenceau, E., Van Der Merwe, P., and Dehairs, F.: Carbon export in the naturally iron-fertilized Kerguelen area of the Southern Ocean based on the ^{234}Th approach, *Biogeosciences Discuss.*, 11, 15991–16032, doi:10.5194/bgd-11-15991-2014, 2014.

Pollard, R., Sanders, R., Lucas, M., and Statham, P.: The Crozet natural iron bloom and export experiment (CROZEX), *Deep-Sea Res. Pt. II*, 54, 1905–1914, doi:10.1016/j.dsr2.2007.07.023, 2007.

Pollard, R. T., Slater, I., Sanders, R. J., Lucas, M. I., Moore, C. M., Mills, R. A., Statham, P. J., Allen, J. T., Baker, A. R., Bakker, D. C. E., Charette, M. A., Fielding, S., Fones, G. R., French, M., Hickman, A. E., Holland, R. J., Hughes, J. A., Jickells, T. D., Lampitt, R. S., Morris, P. J., Nédélec, F. H., Nielsdottir, M., Planquette, H., Popova, E. E., Poulton, A. J., Read, J. F., Seeyave, S., Smith, T., Stinchcombe, M., Taylor, S., Thomalla, S., Venables, H. J., Williamson, R., and Zubkov, M. V.: Southern Ocean deep-water carbon export enhanced by natural iron fertilization, *Nature*, 457, 577–580, doi:10.1038/nature07716, 2009.

Quéguiner, B.: Iron fertilization and the structure of planktonic communities in high nutrient regions of the Southern Ocean, *Deep-Sea Res. Pt. II*, 90, 43–54, 2013.

Sackett, O., Armand, L., Beardall, J., Hill, R., Doblin, M., Connelly, C., Howes, J., Stuart, B., Ralph, P., and Heraud, P.: Taxon-specific responses of Southern Ocean diatoms to Fe en-

Biological productivity regime and associated N cycling

A. J. Cavagna et al.

Title Page

Abstract

Introduction

Conclusions

References

Tables

Figures



Back

Close

Full Screen / Esc

Printer-friendly Version

Interactive Discussion



richment revealed by synchrotron radiation FTIR microspectroscopy, *Biogeosciences*, 11, 5795–5808, doi:10.5194/bg-11-5795-2014, 2014.

Sambrotto, R. N. and Mace, B. J.: Coupling of biological and physical regimes across the Antarctic Polar Front as reflected by nitrogen production and recycling, *Deep-Sea Res. Pt. II*, 47, 3339–3367, 2000.

Sarmiento, J. L., Gruber, N., Brzezinski, M. A., and Dunne, J. P.: High-latitude controls of thermocline nutrients and low latitude biological productivity, *Nature*, 427, 56–60, 2004.

Sarthou, G., Timmermans, K. R., Blain, S., and Tréguer, P.: Growth physiology and fate of diatoms in the oceans: a review, *J. Sea Res.*, 53, 25–42, 2005.

Sarthou, G., Vincent, D., Christaki, U., Obernosterer, I., Timmermans, K. R., and Brussaard, C. P. D.: The fate of biogenic iron during phytoplankton bloom induced by natural fertilization: impact of copepod grazing, *Deep-Sea Res. Pt. II*, 55, 734–751, 2008.

Savoie, N., Dehairs, F., Elskens, M., Cardinal, D., Kopczynska, E. E., Trull, T. W., Wright, S., Baeyens, W., and Griffiths, B. F.: Regional variation of spring N-uptake and new production in the Southern Ocean, *Geophys. Res. Lett.*, 31, 841–855, 2014.

Savoie, N., Trull, T. W., Jacquet, S. H. M., Navez, J., and Dehairs, F.: ²³⁴Th-based export fluxes during a natural iron fertilization experiment in the Southern Ocean (KEOPS), *Deep-Sea Res. Pt. II*, 55, 841–855, 2008.

Sigman, D. M., Altabet, M. A., McCorkle, D. C., Francois, R., and Fischer, G.: The $\delta^{15}\text{N}$ of nitrate in the Southern Ocean: consumption of nitrate in surface waters, *Global Biogeochem. Cy.*, 13, 1149–1166, 1999.

Sigman, D. M., Casciotti, K. L., Andreani, M., Barford, C., Galanter, M., and Böhlke, J. K.: A bacterial method for the nitrogen isotopic analysis of nitrate in seawater and freshwater, *Anal. Chem.*, 73, 4145–4153, 2001.

Smetacek, V., Klaas, C., Strass, V. H., Assmy, P., Montresor, M., Cisewski, B., Savoie, N., Webb, A., d'Ovidio, F., Arrieta, J. M., Bathmann, U., Bellerby, R., Berg, G. M., Croot, P., Gonzalez, S., Henjes, J., Herndl, G. J., Hoffmann, L. J., Leach, H., Losch, M., Mills, M. M., Neill, C., Peeken, I., Röttgers, R., Sachs, O., Sauter, E., Schmidt, M. M., Schwartz, J., Terbrüggen, A., and Wolf-Gladrow, D.: Deep carbon export from a Southern Ocean iron-fertilized diatom bloom, *Nature*, 487, 313–319, doi:10.1038/nature11229, 2012.

Sokolov, S. and Rintoul, S. R.: On the relationship between fronts of the Antarctic Circumpolar Current and surface chlorophyll concentration in the Southern Ocean, *J. Geophys. Res.*, 112, C07030, doi:10.1029/2006JC004072, 2007.

Biological productivity regime and associated N cycling

A. J. Cavagna et al.

Title Page

Abstract

Introduction

Conclusions

References

Tables

Figures

◀

▶

◀

▶

Back

Close

Full Screen / Esc

Printer-friendly Version

Interactive Discussion



Takahashi, T., Sutherland, S. C., Wanninkhof, R., Sweeney, C., Feely, R. A., Chipman, D. W., Hales, B., Friederich, G., Chavez, F., Sabine, C., Watson, A., Bakker, D. C. E., Schuster, U., Metzl, N., Yoshikawa-Inoue, H., Ishii, M., Midorikawa, T., Nojiri, Y., Körtzinger, A., Steinhoff, T., Hoppema, M., Olafsson, J., Arnarson, T. S., Tilbrook, B., Johannessen, T., Olsen, A., Bellerby, R., Wong, C. S., Delille, B., Bates, N. R., and de Baar, H. J. W.: Climatological mean and decadal change in surface ocean $p\text{CO}_2$ and net sea–air CO_2 flux over global oceans, *Deep-Sea Res. Pt. II*, 56, 554–577, 2009.

Timmermans, K. R., Veldhuis, M. J. W., Laan, P., and Brussaard, C. P. D.: Probing natural iron fertilization near the Kerguelen (Southern Ocean) using natural phytoplankton assemblages and diatom cultures, *Deep-Sea Res. Pt. II*, 55, 693–705, 2008.

Waldron, H. N., Attwood, C. G., Probyn, T. A., and Lucas, M. I.: Nitrogen dynamics in the Bellingshausen Sea during the Austral spring of 1992, *Deep-Sea Res. Pt. II*, 42, 1253–1276, 1995.

Ward, B. B.: Nitrogen cycling in aquatic environments, in: *Manual of Environmental Microbiology*, edited by Hurst, C. J., Crawford, R. L., Garland, J. L., Lipson, D. A., Mills, A. L., Stetzenbach, L. D., American Society for Microbiology, 511–522, 2007.

Ward, B. B.: Nitrification in the ocean, in: *Nitrification*, edited by Ward, B. B., Arp, D. J., and Klotz, M. G., American Society of Microbiology, 325–345, 2011.

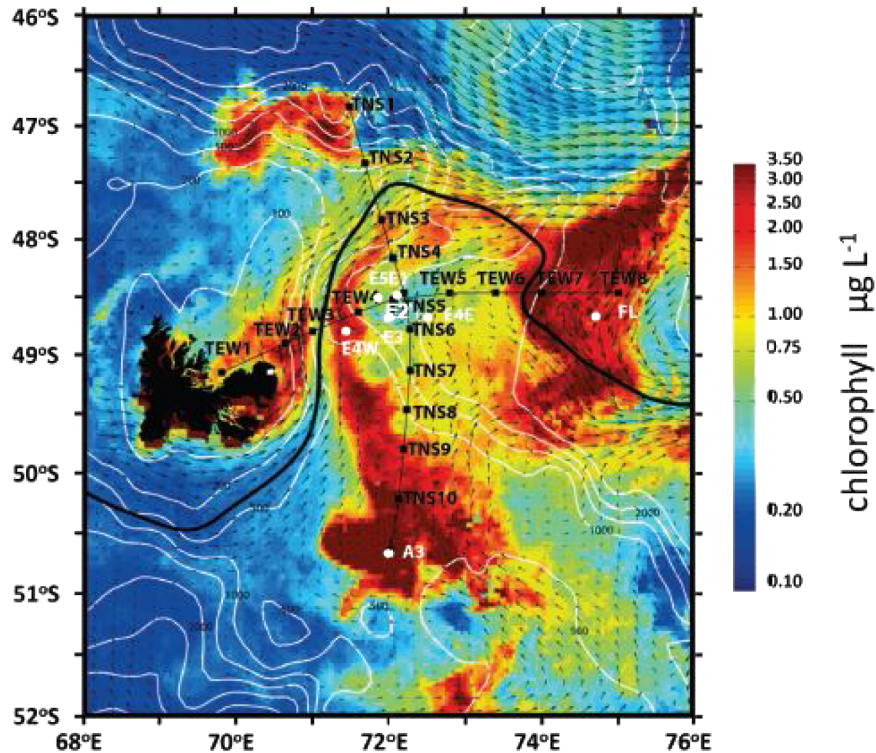


Figure 1. KEOPS2 study area from October to November 2011. Chl *a* (color scale), surface velocity fields (arrows), the polar front (PF, black line), and the position of the different stations (black circles). Stations for which we performed incubations are represented by the white circles: the bloom stations over the Kerguelen plateau (E4-W and A3-2) and North of the Polar Front (F-L); and the meander stations (E stations). The reference HNLC station (R2) is not shown as it is out of the area of the map (Long. East 66.69, Lat. South 50.39). Note that the Chl *a* concentrations correspond to the last week of the KEOPS2 cruise. Courtesy of Y. Park and colleagues.

Biological productivity regime and associated N cycling

A. J. Cavagna et al.

Title Page	
Abstract	Introduction
Conclusions	References
Tables	Figures
◀	▶
◀	▶
Back	Close
Full Screen / Esc	
Printer-friendly Version	
Interactive Discussion	



Biological productivity regime and associated N cycling

A. J. Cavagna et al.

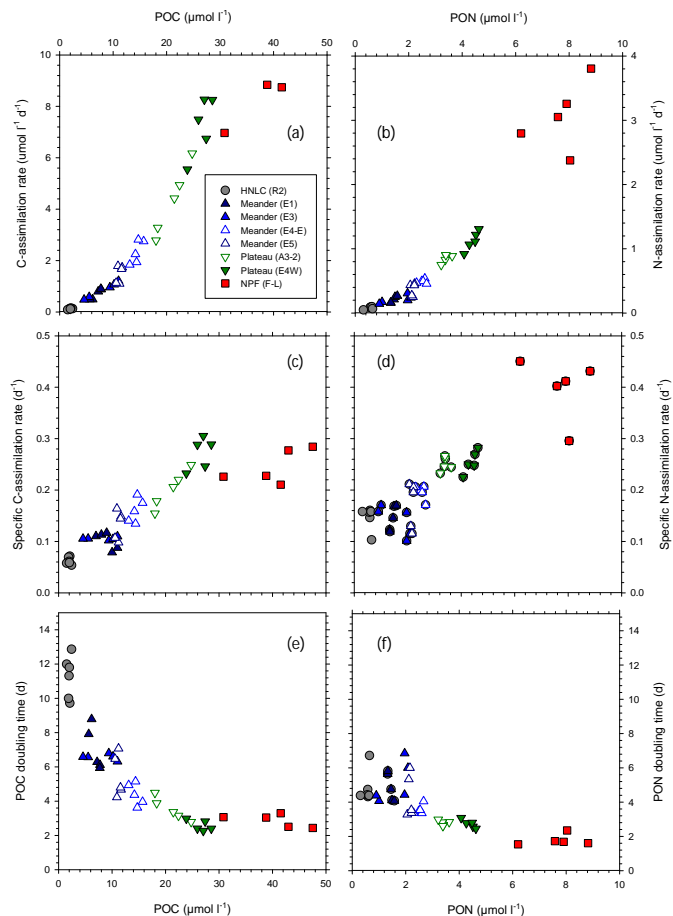


Figure 2. Euphotic layer (100 to 1 % PAR) relationship between POC, PON ($\mu\text{mol L}^{-1}$) and net primary production ($\mu\text{mol C m}^{-2} \text{d}^{-1}$) and N-assimilation rates ($\mu\text{mol N m}^{-2} \text{d}^{-1}$) (a, b), specific C and N assimilation rates (Growth rate; d^{-1}) (c, d), and POC/PON doubling time (e, f).

Biological productivity regime and associated N cycling

A. J. Cavagna et al.

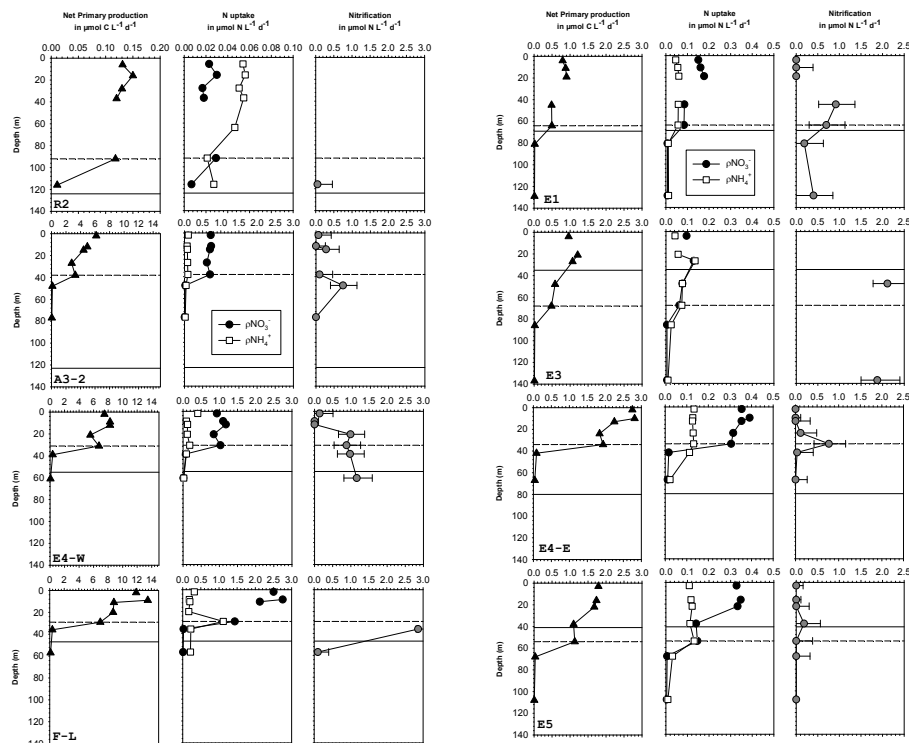


Figure 3. Vertical distribution of net primary production (left column), N-uptake (middle column), and nitrification (right column; error bar corresponding to the 5 and 95 % percentiles) rates between stations (rows). The dashed line represents the euphotic layer depth and the full line the mixed layer depth.

Title Page

Abstract

Introduction

Conclusions

References

Tables

Figures

◀

▶

◀

▶

Back

Close

Full Screen / Esc

Printer-friendly Version

Interactive Discussion

Biological productivity regime and associated N cycling

A. J. Cavagna et al.

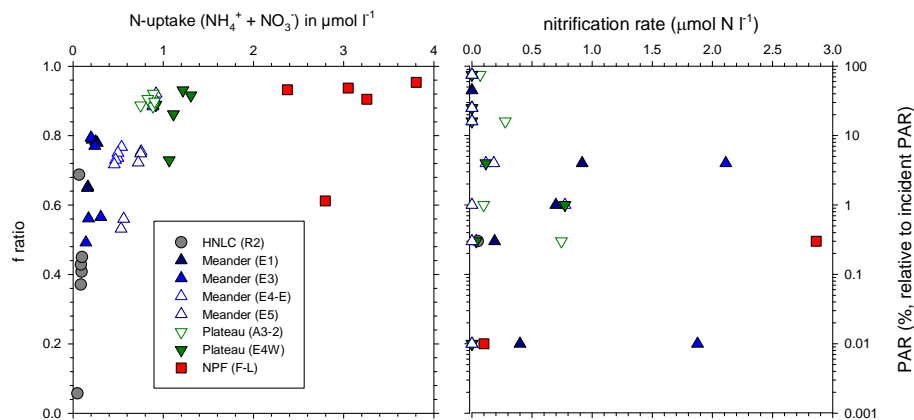


Figure 4. Relationship between N uptake ($\text{NH}_4^+ + \text{NO}_3^-$) and *f* ratio in the euphotic layer (between 100 and 1% PAR) (a), and between PAR(%) and nitrification rates (b).

Title Page

Abstract

Introduction

Conclusions

References

Tables

Figures

◀

▶

◀

▶

Back

Close

Full Screen / Esc

Printer-friendly Version

Interactive Discussion



Biological productivity regime and associated N cycling

A. J. Cavagna et al.

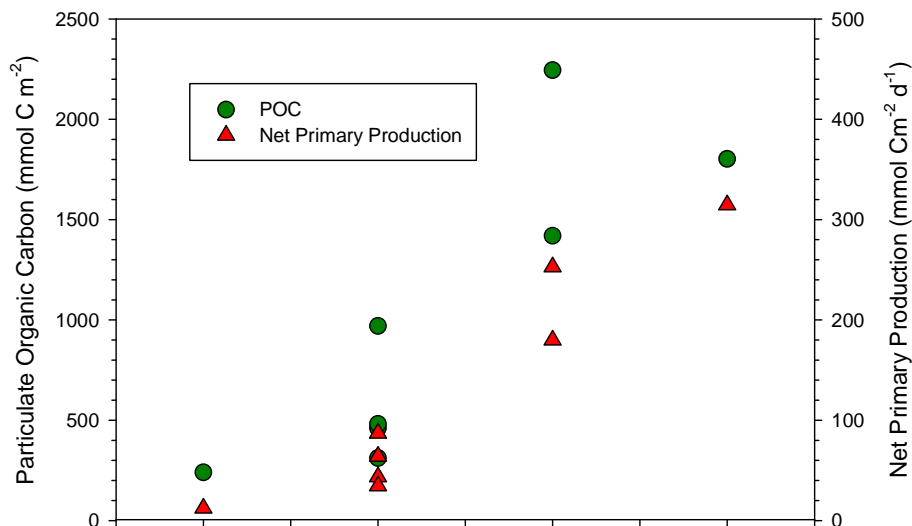


Figure 5. Integrated particulate organic carbon (mmol C m^{-2}) and net primary production ($\text{mmol C m}^{-2} \text{d}^{-1}$) over the mixed layer depth for the different stations: HNLC (R2 station); Plateau (A3-2 and E-4W stations); Meander (E stations); and North of the Polar Front (F-L station).

Title Page

Abstract

Introduction

Conclusions

References

Tables

Figures

⏪

⏩

◀

▶

Back

Close

Full Screen / Esc

Printer-friendly Version

Interactive Discussion



Biological productivity regime and associated N cycling

A. J. Cavagna et al.

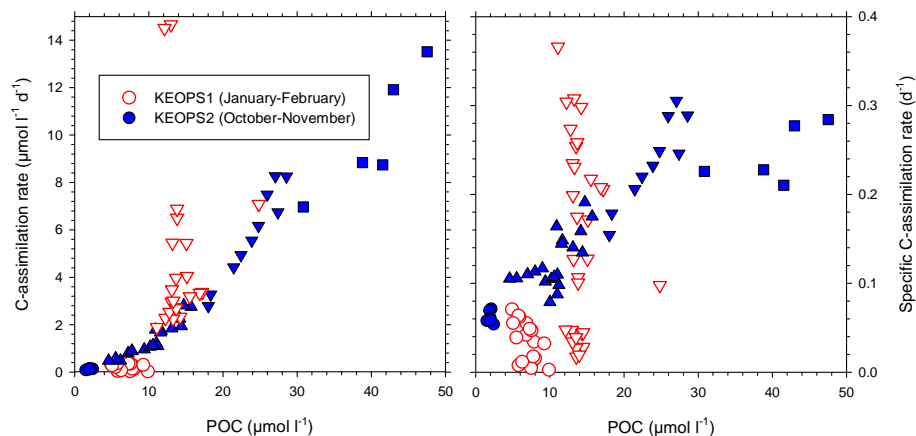


Figure 6. Relationship in the euphotic layer (100 to 1% PAR) between biomass (POC) and net primary production (a), and specific C assimilation rates (Growth rate) (b). The KEOPS2 stations are represented in blue, with the same symbols than in Fig. 1, and KEOPS1 station in red (Raimbault, unpub. results). Inversed red triangles represent the stations over the Kerguelen Southeast Plateau, the red circle the HNLC area east of the plateau (not sampled during KEOPS2).

Title Page

Abstract

Introduction

Conclusions

References

Tables

Figures

◀

▶

◀

▶

Back

Close

Full Screen / Esc

Printer-friendly Version

Interactive Discussion

